**Do-Hyun Lee**[1]
**Je-Kyun Park**[1,2]

[1]Department of Bio and Brain Engineering, Korea Advanced Institute of Science and Technology (KAIST), Yuseong-gu, Daejeon, Republic of Korea
[2]KAIST Institute for the NanoCentury, Yuseong-gu, Daejeon, Republic of Korea

Received June 15, 2013
Revised August 7, 2013
Accepted August 11, 2013

Research Article

# Reduction in microparticle adsorption using a lateral interconnection method in a PDMS-based microfluidic device

Microparticle adsorption on microchannel walls occurs frequently due to nonspecific interactions, decreasing operational performance in pressure-driven microfluidic systems. However, it is essential for delicate manipulation of microparticles or cells to maintain smooth fluid traffic. Here, we report a novel microparticle injection technique, which prevents particle loss, assisted by sample injection along the direction of fluid flow. Sample fluids, including microparticles, mammalian (U937), and green algae (*Chlorella vulgaris*) cells, were injected directly via a through hole drilled in the lateral direction, resulting in a significant reduction in microparticle attachment. For digital microfluidic application, the proposed regime achieved a twofold enhancement of single-cell encapsulation compared to the conventional encapsulation rate, based on a Poisson distribution, by reducing the number of empty droplets. This novel interconnection method can be straightforwardly integrated as a microparticle or cell injection component in integrated microfluidic systems.

**Keywords:**
Cell injection / Droplet-based microfluidics / Lateral interconnection / Particle adsorption / Single-cell encapsulation DOI 10.1002/elps.201300274

## 1 Introduction

In response to the growing demand for miniaturized analytical systems, the microfluidic systems have been widely used in the fields of biology, chemistry, and nanotechnology [1]. In particular, a technique for generation of cell-containing nanoliter droplets improves manipulation and screening capabilities to facilitate high-throughput analysis [2–6]. Most droplet-based microfluidic devices have been fabricated from a hydrophobic polymer, PDMS [7, 8], by a rapid prototyping method, which is widely used due to its high biocompatibility, good optical transparency, and compatibility with lab-on-a-chip techniques. The strong antipathy of water to the hydrophobic wall is an attractive attribute and facilitates the formation of stable droplets. However, there are significant opportunities for the adsorption of organic solvents, small molecules, and particles around the channel inlet due to the innate hydrophobic nature of PDMS microchannels [9]. Nonspecific interactions, such as hydrophobic and Van der Waal's interactions, between particles and the microchannel wall are major causes of reduced reliability and functionality in PDMS-based microfluidic devices.

To address the above issue, various strategies for prevention and elimination of biofouling have been introduced. In particular, in situ surface modification of PDMS microchannels is commonly carried out by chemical treatments using self-assembled monolayer coatings [10–12]. However, the main shortcoming of these methods is that there is no guarantee of uniform coating and durability. For example, their use may result in undesirable reactions when surfactants (e.g. Tween 20 and Pluronic solution) react with an oil phase. The unwanted debris generated by the reaction causes clogging, which interrupts particle movement and decreases cell encapsulation efficiency. Particularly in the process of additive pretreatment, it is urged to take precautions to remove as much excess additives prior to injecting microparticles or cells, due to the hardening of additive that can result in the clogging of microchannels [13]. The rapid recovery of the original hydrophobicity within several minutes to several hours is also a critical drawback for long-term microfluidic studies. Interestingly, electrohydrodynamic buoyancy can be used for removal of adherent particles. Kim et al. [14] proposed a wall loss reduction technique operated by an AC electric potential from interdigitated electrodes integrated at the bottom of the microchannel. Kim et al. [15] reported a method for nanofabricating polyethylene glycol hydrogels on the microchannel surface to improve surface hydrophobicity. Although they showed impressive results, complicated electrode structures

**Correspondence:** Professor Je-Kyun Park, Department of Bio and Brain Engineering, KAIST, 291 Daehak-ro, Yuseong-gu, Daejeon 305-701, Korea
**E-mail:** jekyun@kaist.ac.kr
**Fax:** +82-42-350-4310

**Colour Online:** See the article online to view Figs. 1, 3, 5 and 6 in colour.

 

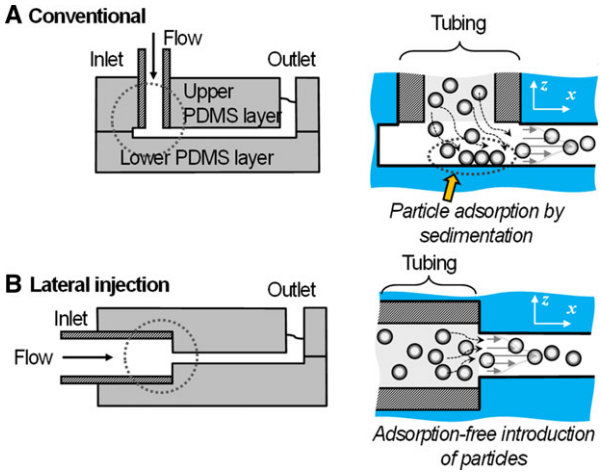


**Figure 1.** A schematic cross-sectional drawing of (A) the conventional PDMS-based microfluidic device and (B) the proposed microfluidic device for microparticle injection. In the proposed device, the plastic tubing is connected to the well-defined interconnection through the side of the PDMS microfluidic device in the same direction as the fluid flow. In this regime, the laterally injected microparticles or cells are directed into the middle of the fluid stream, which is free of both the settling force and nonspecific surface–particle interactions.

and intensive fabrication processes were required, which limits its application in integrated microsystems.

Since encapsulation into droplets follows a Poisson distribution [16], surface fouling results in a decrease in particle encapsulation efficiency due to the higher rate of empty droplets relative to positive droplets. The occasional clogging by adsorption at the narrow constriction also provokes inefficient particle loading in drops. This inefficiency has been improved by deterministic single-cell encapsulation within droplets using inertial ordering with a high flow rate [2, 17]. Despite the high yield of single-cell encapsulation, there is an increased possibility of cell damage due to the high shear rate. In addition, the high pressure would result in fluid leakage at the inlets due to fluidic resistance.

In the former approach, a through-hole type interconnection for particle injection, the plastic tubing was penetrated and connected through inlet holes that were perpendicular to the flow direction [18–20]. As the flow was injected, the settling force around the inlet would be increased, and thus particle adhesion would be aggravated by particle sedimentation (Fig. 1A). Introduction of sample fluid, including microparticles or cells, with a high flow rate may contribute to prevention of particle adhesion, but it is difficult to tune the low droplet frequency and control the droplet size accurately at such high flow rates. Solvas et al. [21] utilized a mini-magnetic stirrer to stir the cell suspensions within a commercial syringe that contained a tiny magnetic stir bar. However, this method cannot guarantee prevention of particle adhesion around the microfluidic inlet. As a remedy for the adsorption problem, we propose a novel interconnection approach assisted by lateral injection of the sample fluid via a direct side interconnection (Fig. 1B). The inlet holes connected to a syringe tube are easily punched through the side of the microfluidic device in the same direction as the fluid flow. Several other methods have already been described for delivering fluid laterally into silicon-based microfluidic channels using complex fabrication methods [22, 23] or into PDMS-based microfluidic channels through a glass capillary [24], but no attempts have been made to realize the well-defined interconnection through the side of the PDMS microfluidic device with a simple fabrication process to connect the plastic tube. This simple punching method contributes to the well-defined interconnection through the side of the PDMS microfluidic device. In addition, the defined interconnection holes can be fabricated quickly and robustly irrespective of the complexity of the microfluidic network. By connecting the injection tube to the defined holes directly, we demonstrate smooth introduction of microparticles or cells with reduced particle adsorption. In addition, we present a significant application to emphasize the advantageous points of the digital microfluidics such as the encapsulation of single cells in microdroplets. This microparticle injection method reduces the number of empty droplets while increasing the single-cell encapsulation efficiency.

## 2 Materials and methods

### 2.1 Design and fabrication

Figure 2 shows a schematic diagram of the overall process for fabrication of the microfluidic device with lateral interconnections. A microfluidic device was fabricated using a conventional PDMS (Sylgard 184; Dow Corning, Midland, MI, USA) molding process. The mold for the PDMS replica was fabricated by SU-8 patterning on a silicon wafer. For microparticle applications, the channels were 100 μm in width and 35 μm in thickness. The outlets for fluid collection were

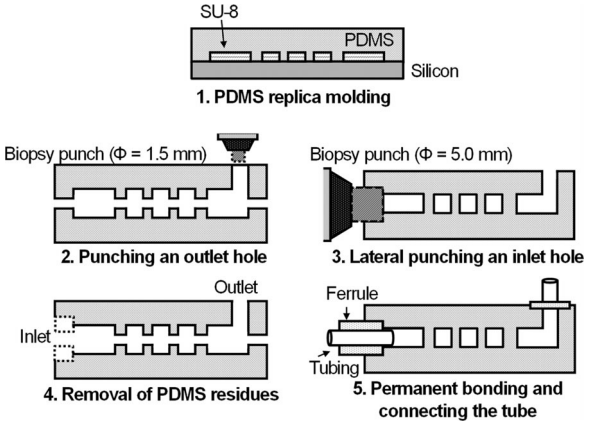


**Figure 2.** A schematic diagram of the overall process for fabrication of the microfluidic device with lateral interconnections. The defined interconnect holes were robustly fabricated in a lateral direction using a biopsy punch with a diameter of 5.0 mm. After removal of the PDMS fragment, the microfluidic ferrule was assembled into the punched inlet port to improve the alignment and achieve perfect sealing.

 

punched out using a punch with a diameter of 1.5 mm (Harris Uni-Core Punch; Ted Pella, Redding, CA, USA). A PDMS layer with microchannels and another PDMS layer reversibly faced each other. Then, the inlet hole was punched at the side of the faced device in a lateral direction using a punch with a diameter of 5.0 mm. Direct insertion of the needle into the side of the microfluidic device may give rise to inaccurate penetration and damage the PDMS around the punched site. This structural mismatch would lead to unexpected leakage around the inlet. In addition, to embed the ferrule successfully, the thickness of the whole PDMS device should be greater than 6 mm.

The residual PDMS fragment was removed using a pair of tweezers. To align and permanently bond the PDMS replicas, each layer was treated with an oxygen plasma. To form a perfect seal against the side of the microfluidic device and Tygon tubing (0.06″ od, Tygon R-AAQ04103; Saint-Gobain Performance Plastics, Akron, OH, USA), we used a commercially available microfluidic ferrule (Flangeless Ferrule PK10 P-200NX for 1/16″ od tubing; Upchurch, Oak Harbor, WA, USA). The ferrule, which had an outer diameter of 0.46 cm and a length of 0.56 cm, was assembled into the punched inlet port (diameter, 5.0 mm). After casting uncured PDMS around the ferrule and inlet port, the microfluidic device was stored at 70°C for 1 h. This curing process supports robust fixation of the ferrule without fluid leakage. To avoid wetting of the PDMS microchannel by an aqueous phase, the microchannel was flushed with an oil phase before introduction of an aqueous phase.

### 2.2 Materials

Solutions of red food dye (Kemide Co., Jeonju, Korea) were used to visualize the fluid introduction. Fluorescein isothiocyanate solution (Sigma-Aldrich, St. Louis, MO, USA) with a concentration of 50 μg/mL was prepared. Red fluorescent polystyrene beads with a diameter of 15 μm were purchased from Invitrogen Corporation (Carlsbad, CA, USA). The beads were prepared in 6% Pluronic F68 solution (Sigma-Aldrich) at a concentration of approximately $5 \times 10^5$/mL. For droplet-generation experiments, a continuous oil phase used was mineral oil (Sigma-Aldrich) without surfactants.

The human histolytic lymphoma monocyte (U937) cell line was cultured in RPMI 1640 medium (Invitrogen) supplemented with 10% v/v heat-inactivated fetal bovine serum (Invitrogen), 100 units/mL penicillin G, and 100 g/mL streptomycin. Cell cultures were maintained in a humidified atmosphere containing 5% $CO_2$. Then, cells were centrifuged at 1000 rpm for 3 min to remove the supernatant and stained with 10 M CellTracker Green CMFDA (Molecular Probes, Eugene, OR, USA). *Chlorella vulgaris* cells were precultivated for three days at 20°C in nonsaline BG 11 medium under constant shaking and continuous illumination with a 3000 lux lamp. Suspensions of $1 \times 10^7$ and $5 \times 10^7$ cells/mL were used in the experiments.

### 2.3 Experimental setup

All microparticle-containing fluids were introduced using a syringe pump (KDS200; KD Scientific, Holliston, MA, USA). The trajectories of the fluorescent microparticles were recorded with a charge-coupled device (DS-U1; Nikon Instruments, Melville, NY, USA). The movements of droplets, including single cells, were recorded with a computer-controlled high-speed camera (Hotshot 512sc; NAC Image Technology, Simi Valley, CA, USA) mounted onto an inverted optical microscope (TS100; Nikon, Tokyo, Japan).

## 3 Results and discussion

### 3.1 Leakage-free lateral interconnection using a ferrule-coupled microchannel

A ferrule-coupled inlet port for facile connection of the device to a commercial syringe was constructed successfully. Figure 3A and B shows an image of the fabricated microfluidic device laterally connected to a Tygon tube. The device consists of two layers: one for the microchannel (height, 40 μm) and the other for the nonpatterned slab. The ferrule also has a hollow structure that has a cavity in the central portion, thus the tubing can penetrate the ferrule with a perfect seal and eliminate the dead volume (Fig. 3C). To characterize the performance of the proposed interconnection, we

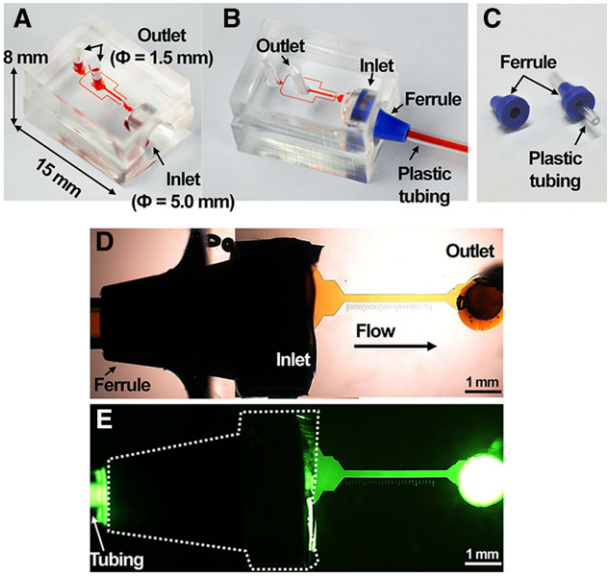


**Figure 3.** Photograph of the fabricated device (A) without and (B) with the microfluidic ferrule and plastic tubing. The device consists of two layers: one for the microchannel (height, 40 μm) and the other for the nonpatterned slab. The microchannels were filled with dye solution to facilitate visualization. (C) Photograph of the ferrule that has a cavity in the central portion. The tubing can penetrate the ferrule with perfect sealing. (D and E) Results of the leakage test. The yellow dye (D) and fluorescein isothiocyanate solution (E) were continuously injected into the linear microchannel.

 

conducted a leakage test as sample fluid was continuously injected into the linear microchannel (Fig. 3D and E). Red dye and fluorescein isothiocyanate solution was placed in a syringe. There was no apparent leakage around the connectors when the fluids were infused directly by pushing the syringe piston using finger force with an approximate flow rate of 6 mL/h. At the same time, the injected fluid was collected continuously at the outlet. Also, the commercial microfluidic ferrule was recyclable and endurable for repetitive manipulations such as insertion or removal of tubings. We confirmed that there was no leakage around the microfluidic ferrule when the tubing was inserted repeatedly more than 30 times.

### 3.2 Microparticle or cell injection using a lateral interconnection method

We verified the reduction in adsorption when microparticles were injected within the microchannel. By enumerating immovable beads 10 min after fluid introduction, we could evaluate the probability of particle adsorption in the conventional and proposed devices. Because the areas for particle/cell counting were different in the two devices, the number of adsorbed particles/cells was normalized to a certain area (1 $mm^2$) of inlet part. As shown in Fig. 4, the number of attached particles per $mm^2$ of surface area was varied according to the flow rate (25–200 μL/h). The number of attached particles was significantly decreased using the proposed microparticle injection method. Despite the relatively low input flow rate, we were able to manipulate most of the introduced microparticles freely. However, at lower flow rates, the adsorption of particles around the inlet was problematic using the conventional approach. These results suggest that most particles settled immediately due to the sedimentation force under low flow rate conditions. Microparticles cannot

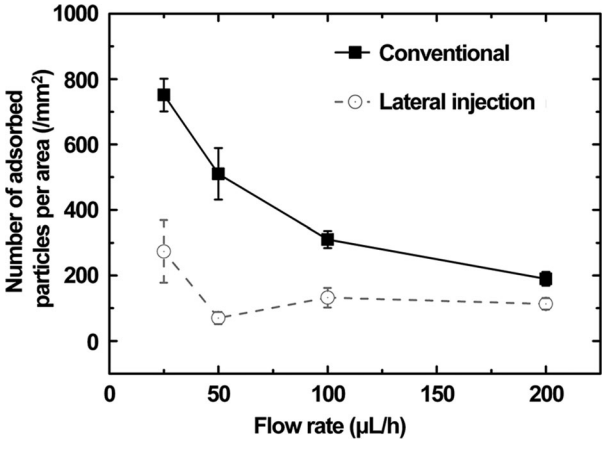


**Figure 4.** Plot of attached microparticle number per $mm^2$ of surface area according to the input flow rate in the conventional and proposed microfluidic devices. In the proposed microfluidic device, we were able to manipulate freely most of the introduced microparticles without attachment around the inlet, despite the relatively low input flow rate.

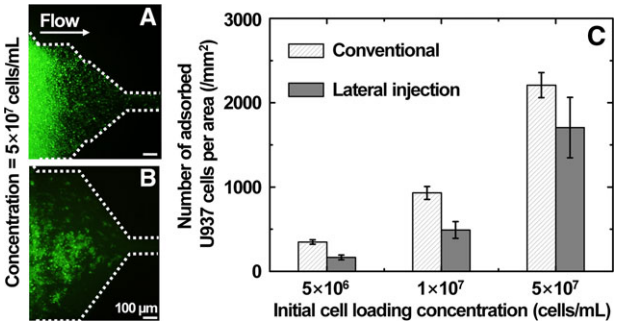


**Figure 5.** Reduction of mammalian cell attachment by lateral injection. Fluorescence images of attachment of U937 cells around the inlet of the (A) conventional and (B) proposed microfluidic device upon loading of $5 \times 10^7$ cells/mL. (C) Plot of the attached cell number per $mm^2$ of surface area according to the initial cell loading concentration. The number of attached cells was markedly decreased by use of the proposed method, and the difference in cell attachment between the two methods decreased with increasing cell loading concentration.

be manipulated once they are attached to the PDMS surface. This is critical for loading of single particles or cells into the droplets.

We also confirmed injection of U937 cells according to the initial cell loading concentration using both the conventional and proposed methods (Fig. 5). To quantify cell attachment, the number of adsorbed U937 cells per $mm^2$ of surface area was considered for each of the two methods. The input flow rate was maintained at 25 μL/h. Using the conventional method, the numbers of adsorbed cells were 347 ± 7, 930 ± 76, and 2208 ± 148 for injected cell concentrations of $5 \times 10^6$, $1 \times 10^7$, and $5 \times 10^7$ cells/mL, respectively. In contrast, using the proposed method, the numbers of adsorbed cells for the same injected cell concentrations were 164 ± 28, 490 ± 99, and 1705 ± 358, respectively. Thus, the number of attached cells was markedly decreased using the proposed method, and the difference in cell attachment between the two methods decreased with increasing cell loading concentration. This is because cell–cell and cell–surface interactions would be enhanced with increasing cell concentrations. This result suggests that introduction of cells with minimal cell loss could be achieved using a lower concentration of cells than with the conventional injection method. This novel approach may thus be useful for continuous separation and isolation of rare cell types.

For further evaluation of time-lapse cell attachment within the proposed device, the conventional (Fig. 6A) and proposed methods (Fig. 6B) were compared with regard to continuous cell loading in a straight microchannel with an input flow rate of 200 μL/h. The green microalga, *C. vulgaris*, which is of great interest for second-generation biofuels [25], was tested. While most of the adsorbed cells accumulated around the plastic tube in the conventional microfluidic device, few cells were adsorbed in the proposed microfluidic device. Previously attached cells could exacerbate cell accumulation due to cell–cell interactions, which may result in channel clogging upon long-term introduction of fluid.

 

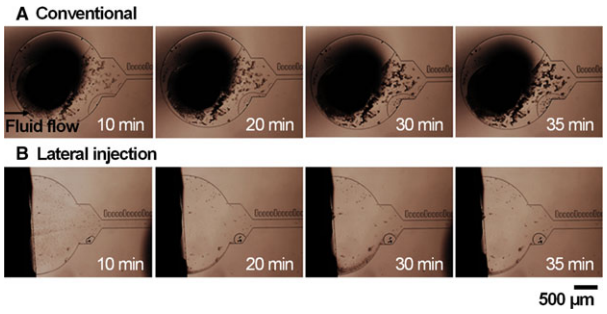


**Figure 6.** Continuous loading of *C. vulgaris* cells into the linear microchannel with injection times of 10–35 min using the (A) conventional and (B) proposed methods. While most of the adsorbed cells were accumulated around the plastic tube in the conventional microfluidic device, few cells were adsorbed in the proposed microfluidic device.

However, in the proposed microfluidic device, channel clogging due to cell accumulation did not occur around the inlet until 35 min after fluid introduction, indicating that the proposed injection method is more robust for long-term microfluidic applications. Unexpectedly, entrapped air bubbles were observed around the inlet, but did not affect device performance (Fig. 6). Therefore, we believe that our system is useful as an experimental platform for efficient cell injection irrespective of cell size for several cell manipulation applications.

Several modular approaches to building integrated modular microfluidic systems have been developed recently [26]. For fastening and bonding of the microfluidic modules with each other, the up-and-down connection approach was utilized as a breadboard. This approach suffers from an increased duration of sample passage, which leads to both extra time being required for sample transportation and the existence of a dead volume. However, using the proposed interconnection, leakage-free interconnections together with various microfluidic modules may facilitate miniaturization of the interconnection components by reducing the space required.

### 3.3 Droplet-based single-cell encapsulation

For practical purposes, this microfluidic approach was used to encapsulate single cells into monodispersed droplets with improved efficiency. In particular, screening of lipid-abundant microalgae, such as *C. vulgaris*, requires appropriate cell culture techniques and single-cell encapsulation strategies. Various droplet-based microfluidic platforms have been used to enhance single-cell encapsulation efficiency, such as hydrodynamic self-sorting [27], close-packed [28], and deterministic ordering of cells [2, 17]. However, these methods require an additional flow, specific microchannel dimensions, a high input flow rate, and compact loading of the cells at higher concentrations. Thus, the intrinsic problem of cell attachment, which leads to cell loss, could not be solved. The reduction in the number of attached cells that resulted from the use of

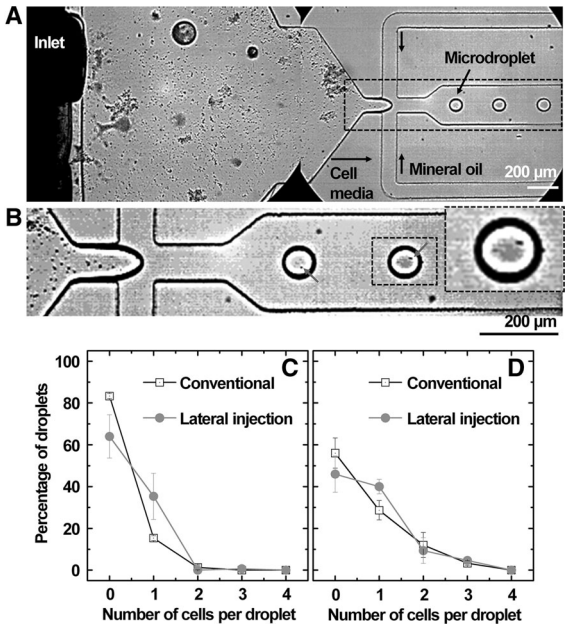


**Figure 7.** (A) The lateral injection of *C. vulgaris* cells at an initial cell loading concentration $5 \times 10^7$/mL in the direction of flow led to the generation of single-cell droplets. (B) Enlargement of the microscopy image of single-cell encapsulation. Gray arrows indicate droplets encapsulating single cell. (C and D) Percentage of droplets containing single cells according to the initial cell loading concentration, (C) $1 \times 10^7$ and (D) $5 \times 10^7$ cells/mL, in the conventional and proposed microfluidic devices.

the proposed injection method is critical for determining the efficiency of single-cell encapsulation into droplets [29].

We compared the percentage of droplets containing single cells under two different initial cell-loading conditions ($1 \times 10^7$ and $5 \times 10^7$ cells/mL) collected at the outlet of the conventional and proposed microfluidic devices. For generation of droplets ~60 μm in diameter, the oil phase and cell culture medium flow rates were 200 and 25 μL/h, respectively (Fig. 7A). Using the conventional method, the distribution of encapsulation efficiency was similar to the Poisson distribution, which yields a higher percentage of empty droplets than those containing multiple cells. The ratio of single-cell droplets did not exceed 30% regardless of the cell concentration used, and the percentage of cell-containing droplets decreased as the initial cell-loading conditions decreased. In contrast, our cell injection method was effective in reducing the percentage of empty droplets, which was due to the reduction of cell attachment, and also resulted in an increase in the percentage of single-cell-containing droplets. Figure 7B shows an enlarged view of a microscopic image of single-cell encapsulation. At a lower concentration ($1 \times 10^7$ cells/mL), there was a noticeable decrease in the percentage of empty droplets, leading to an increase in the percentage of those containing single cells from 15.33 ± 1.15% to 35.33 ± 11.02% ($n = 3$) (Fig. 7C). As shown in Fig. 7D, at the high concentration of $5 \times 10^7$ cells/mL, the fraction of droplets containing single cells increased gradually from 28.67 ± 4.62% to 40.00 ± 3.46% ($n = 3$).

 

To enhance the single-cell encapsulation efficiency compared with the conventional method based on Poisson statistics, we significantly reduced cell adhesion by weakening the vertical settling force using the proposed method. The ratio of cell-encapsulating droplets (including single- and multiple-cell droplets) increased from 17 to 36% at a lower concentration ($1 \times 10^7$ cells/mL), and 44 to 54% at a higher concentration ($5 \times 10^7$ cells/mL). Also, the ratio of empty droplets was markedly decreased at the lower concentration of $1 \times 10^7$ cells/mL. However, an increase in the initial cell concentration resulted in two negative effects on single-cell encapsulation into droplets. First, as mentioned previously, if the initial loading concentration was high, the effects of cell–cell and cell–surface interactions were dominant. The cells already attached to the microchannel surface trigger cell–cell adhesion and form cell aggregates, thus hindering the smooth introduction of cells around the microfluidic inlet. This implies that the increase in the cell-encapsulating droplet ratio was relatively low at the higher concentration of $5 \times 10^7$ cells/mL. Second, according to the Poisson distribution, the number of multiple-cell droplets also increased with increasing initial cell-loading concentration. The same phenomenon occurred in the proposed device due to the large number of cells loaded. Further efforts should focus on reducing the fraction of multiple-cell droplets by integrating microfluidic droplet separation components.

## 4 Concluding remarks

We developed a new microfluidic interconnection for microparticle injection, which utilizes lateral flow in a PDMS-based microfluidic device for preventing particle loss. The lateral movement of the microparticles or cells through the inlet holes that were robustly and accurately punched into the side of a double-layer PDMS microfluidic device resulted in significant reduction in nonspecific adsorption to microchannel walls without any surface modification. With this method, single-cell encapsulation into monodispersed microdroplets was successfully demonstrated and yielded a twofold enhancement of efficiency due to the reduced percentage of empty droplets. This inexpensive, easy, reusable, and high-integrity interconnection technology will be practical for design of microfluidic systems for a number of biomedical applications, such as microfluidic cell culture, isolation of rare cell types, and single-cell encapsulation within microdroplets. Furthermore, the proposed interconnection could be coupled with other microfluidic cell-sorting systems, such as a fluorescence-activated cell sorter [30], magnet-activated cell sorter [31], or fluorescence-activated droplet sorter [32], to enhance both purity and recovery rate by reducing sample loss.

*This research was supported by a National Leading Research Laboratory Program (grant number NRF-2013R1A2A1A05006378), a Nano/Bio Science and Technology Program (grant number 2011-0002188), and a Converging Research Center Program (grant number 2011K000864) through the National Research Foundation of Korea funded by the Ministry of Science, ICT, and Future Planning. The authors thank Professor Jong-In Han for preparation of algal cells and helpful discussion. We also thank Chae Yun Bae for mammalian cell culture and preparation.*

*The authors have declared no conflict of interest.*

## 5 References

[1] Janasek, D., Franzke, J., Manz, A., *Nature* 2006, *442*, 374–380.

[2] Edd, J. F., Di Carlo, D., Humphry, K. J., Köster, S., Irimia, D., Weitz, D. A., Toner, M., *Lab Chip* 2008, *8*, 1262–1264.

[3] Köster, S., Angile, F. E., Duan, H., Agresti, J. J., Wintner, A., Schmitz, C., Rowat, A. C., Merten, C. A., Pisignano, D., Griffiths, A. D., Weitz, D. A., *Lab Chip* 2008, *8*, 1110–1115.

[4] Moon, S., Kim, Y. G., Dong, L., Lombardi, M., Haeggstrom, E., Jensen, R. V., Hsiao, L. L., Demirci, U., *PLoS One* 2011, *6*, e17455.

[5] Um, E., Rha, E., Choi, S. L., Lee, S. G., Park, J. K., *Lab Chip* 2012, *12*, 1594–1597.

[6] Chen, Z., Teng, D. H. Y., Wang, G. C. J., Fan, S. K., *BioChip J.* 2011, *5*, 343–352.

[7] Tice, J. D., Song, H., Lyon, A. D., Ismagilov, R. F., *Langmuir* 2003, *19*, 9127–9133.

[8] Duffy, D. C., McDonald, J. C., Schueller, O. J. A., Whitesides, G. M., *Anal. Chem.* 1998, *70*, 4974–4984.

[9] Ocvirk, G., Munroe, M., Tang, T., Oleschuk, R., Westra, K., Harrison, D. J., *Electrophoresis* 2000, *21*, 107–115.

[10] Seo, J. H., Shibayama, T., Takai, M., Ishihara, K., *Soft Matter* 2011, *7*, 2968–2976.

[11] Dou, Y. H., Bao, N., Xu, J. J., Chen, H. Y., *Electrophoresis* 2002, *23*, 3558–3566.

[12] Boxshall, K., Wu, M. H., Cui, Z., Cui, Z., Watts, J. F., Baker, M. A., *Surf. Interface Anal.* 2006, *38*, 198–201.

[13] Teh, S. Y., Khnouf, R., Fan, H., Lee, A. P., *Biomicrofluidics* 2011, *5*, 044113.

[14] Kim, M., Kim, Y. H., Kim, H. L., Park, C. W., Joe, Y. H., Hwang, J., Kim, Y. J., *J. Micromech. Microeng.* 2010, *20*, 035034.

[15] Kim, P., Jeong, H. E., Khademhosseini, A., Suh, K. Y., *Lab Chip* 2006, *6*, 1432–1437.

[16] Clausell-Tormos, J., Lieber, D., Baret, J. C., El-Harrak, A., Miller, O. J., Frenz, L., Blouwolff, J., Humphry, K. J., Köster, S., Duan, H., Holtze, C., Weitz, D. A., Griffiths, A. D., Merten, C. A., *Chem. Biol.* 2008, *15*, 427–437.

[17] Kemna, E. W. M., Schoeman, R. M., Wolbers, F., Vermes, I., Weitz, D. A., van den Berg, A., *Lab Chip* 2012, *12*, 2881–2887.

[18] Bhagat, A. A. S., Jothimuthu, P., Pais, A., Papautsky, I., *J. Micromech. Microeng.* 2007, *17*, 42–49.

[19] Christensen, A. M., Chang-Yen, D. A., Gale, B. K., *J. Micromech. Microeng.* 2005, *15*, 928–934.

[20] Zhu, X., Chu, L. Y., Chueh, B.-H., Shen, M., Hazarika, B., Phadke, N., Takayama, S., *Analyst* 2004, *129*, 1026–1031.

 

[21] Solvas, X. C. I., Niu, X., Leeper, K., Cho, S., Chang, S. I., Edel, J. B., *J. Vis. Exp.* 2011, *58*, e3437.

[22] Gonzalez, C., Collins, S. D., Smith, R. L., *Sens. Actuator B Chem.* 1998, *49*, 40–45.

[23] Gray, B. L., Collins, S. D., Smith, R. L., *Sens. Actuator A Phys.* 2004, *112*, 18–24.

[24] Zheng, B., Gerdts, C. J., Ismagilov, R. F., *Curr. Opin. Struc. Biol.* 2005, *15*, 548–555.

[25] Rodolfi, L., Chini Zittelli, G., Bassi, N., Padovani, G., Biondi, N., Bonini, G., Tredici, M. R., *Biotechnol. Bioeng.* 2009, *102*, 100–112.

[26] Shaikh, K. A., Ryu, K. S., Goluch, E. D., Nam, J. M., Liu, J., Thaxton, C. S., Chiesl, T. N., Barron, A. E., Lu, Y., Mirkin, C. A., *Proc. Natl. Acad. Sci. USA* 2005, *102*, 9745–9750.

[27] Um, E., Lee, S. G., Park, J. K., *Appl. Phys. Lett.* 2010, *97*, 153703.

[28] Abate, A. R., Chen, C. H., Agresti, J. J., Weitz, D. A., *Lab Chip* 2009, *9*, 2628–2631.

[29] Lee, D. H., Lee, W., Um, E., Park, J. K., *Biomicrofluidics* 2011, *5*, 034117.

[30] Fu, A. Y., Chou, H. P., Spence, C., Arnold, F. H., Quake, S. R., *Anal. Chem.* 2002, *74*, 2451–2457.

[31] Sun, L., Zborowski, M., Moore, L. R., Chalmers, J. J., *Cytometry* 1998, *33*, 469–475.

[32] Baret, J. C., Miller, O. J., Taly, V., Ryckelynck, M., El-Harrak, A., Frenz, L., Rick, C., Samuels, M. L., Hutchison, J. B., Agresti, J. J., Link, D. R., Weitz, D. A., Griffiths, A. D., *Lab Chip* 2009, *9*, 1850–1858.

 